Relaxation Oscillations and Pulse Stability in Harmonically Mode-Locked Semiconductor Lasers

Farhan Rana and Paul George

***Abstract*—In this paper, we discuss pulse dynamics in harmonically mode-locked semiconductor lasers and present the conditions necessary for stability. In a laser mode-locked at the Nth harmonic, the pulse energy fluctuations have $(N+1)$ different modes of relaxation oscillations. Different modes correspond to different patterns for the energy fluctuations in the N different pulses inside the laser cavity. In the higher order relaxation oscillation modes, the energy fluctuations are negatively correlated in different pulses inside the laser cavity, and these modes can cause instability. Gain saturation on time scales of the order of the pulse width (dynamic gain saturation) stabilizes pulse energy fluctuations with respect to relaxation oscillations. The precise limits on the stable operating regime depend on the gain dynamics at both slow and fast time scales. We also discuss harmonic mode-locking in the presence of a slow saturable absorber. Dynamic loss saturation in a saturable absorber can work against dynamic gain saturation and limit the stability range for harmonic mode-locking.**

***Index Terms*—Laser stability, optical pulses, semiconductor lasers.**

I. Introduction

HARMONICALLY mode-locked lasers are attractive as sources of high-repetition-rate optical pulses that can be used in electrooptic sampling, optical analog-to-digital conversion, optical telecommunication systems, and ultrafast optical measurements [1]–[5]. Stability of the pulses in harmonically mode-locked lasers is important for most of these applications. A laser mode-locked at the Nth harmonic has N optical pulses propagating inside the laser cavity. The requirements for pulse stability in fiber lasers were analyzed in [6] and [7]. It was shown that pulse stability results from the combination of Kerr nonlinearity and optical filtering. For soliton pulses, the pulse width is inversely proportional to the pulse energy. If the pulse energy increases, the pulse width decreases and the pulse experiences less loss from the active modulator. On the other hand, since the pulse bandwidth also increases with decrease in the pulse width, the pulse experiences more loss from the optical filter. The pulse energy fluctuations are damped if the increase in loss from the optical filter is more than the increase in gain from the active modulator. This condition was used to obtain a minimum value for the pulse energy for stable operation. The stability of soliton pulses in fiber lasers was also analyzed numerically in [8], and the stability requirements predicted in [6] and [7] were verified. It was also shown in [8] that, when the pulse power is smaller than the minimum value required for stable operation, instabilities can lead to pulse dropouts. In the case of harmonically mode-locked semiconductor lasers, the following questions arise: 1) what stabilizes the pulses and 2) what are the limits on the stable operating regime. In this paper, we present a theoretical model to answer these questions.

In the analytical treatments of [6] and [7], it was assumed that every pulse in the laser cavity is the same. This assumption makes it impossible to study the slow gain dynamics and find the precise limits on the stable operating regime. In harmonically mode-locked semiconductor lasers, the gain relaxation times can be much longer than the pulse repetition times. Pulse energy fluctuations that are negatively correlated in different pulses inside the laser cavity do not change the average power much and are therefore almost invisible to the gain medium on slow time scales. These negatively correlated pulse energy fluctuations can grow, causing instability and pulse dropouts. The energy fluctuations in all of the pulses in the laser cavity as well as the gain dynamics need to be taken into account to find the precise limits on the stable operating regime. Harmonically mode-locked semiconductor lasers can have more than 100 different pulses propagating inside the laser cavity [3], [9]–[11], and it seems like a daunting task to numerically model the fluctuations in all of the pulses. The theoretical technique presented in this paper takes into account the energy fluctuations in all of the pulses in the laser cavity as well as the gain dynamics via nonlinear finite-difference equations, which are then linearized to obtain finite-difference equations for the pulse photon-number fluctuations. A similar method was used by the authors earlier to characterize the pulse timing fluctuations in harmonically mode-locked lasers [12].

Pulse stability in fundamentally and harmonically mode-locked semiconductor lasers can be affected by a number of different processes. For example, in [13], it was shown that, in actively mode-locked lasers, dynamic gain saturation in the gain medium causes the pulse to move off the gain maximum (in time) of the modulator, and the excess gain just behind the pulse results in instabilities that limit the maximum pulse energy. In lasers, the oscillatory dynamics of small perturbations in laser gain and photon number around an operating point are called relaxation oscillations. The operating point is considered stable if the perturbations are damped in time. The operating point is unstable if small fluctuations

Manuscript received March 27, 2007; revised July 11, 2007. This work was supported in part by a National Science Foundation Faculty CAREER Award, in part by ILX Lightwave Corporation, in part by Intel Inc., and in part by Infotonics Inc.

The authors are with the School of Electrical and Computer Engineering, Cornell University, Ithaca, NY 14853 USA (e-mail: fr37@cornell.edu; pag25@cornell.edu).

Color versions of one or more of the figures in this paper are available online at http://ieeexplore.ieee.org.

Digital Object Identifier 10.1109/JQE.2007.907261

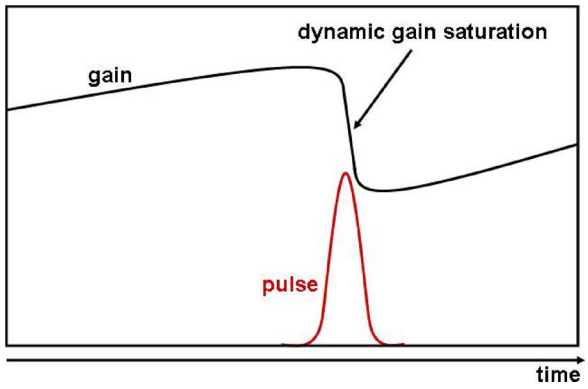

Fig. 1. Dynamic gain saturation in semiconductor gain medium.

grow with time and drive the laser system away from the operating point. In this paper, we focus only on the instabilities that could arise in harmonically mode-locked semiconductor lasers as a result of the dynamics of the nonlinear interaction among the pulses via the gain medium and on the conditions for stability with respect to relaxation oscillations. We show that gain saturation on time scales of the order of the pulse width (dynamic gain saturation) stabilizes pulse energy fluctuations in harmonically mode-locked semiconductor lasers with respect to relaxation oscillations (see Fig. 1). Therefore, Kerr nonlinearity and soliton effects are not necessary for stability in harmonically mode-locked semiconductor lasers. The precise limits on the stable operating regime depend on the gain dynamics at both slow and fast time scales. We show that, in a laser mode-locked at the Nth harmonic, the pulse energy fluctuations have $(N+1)$ different modes of relaxation oscillations. Different modes correspond to different patterns for the energy fluctuations in the N different pulses inside the laser cavity. The lowest two of these modes correspond to the two quadratures of damped relaxation oscillations in which the energies of all of the pulses in the laser cavity fluctuate in phase. In the higher order relaxation oscillation modes, the energy fluctuations are negatively correlated in different pulses inside the laser cavity, and these modes can cause instability. We also discuss harmonic mode-locking in the presence of a slow saturable absorber. Dynamic loss saturation in a saturable absorber can work against dynamic gain saturation and limit the stability range for harmonic mode-locking.

II. Theoretical Model

We consider the external-cavity ring laser topology of [3], [9], and [10] and shown in Fig. 2. The laser structure consists of a gain section [a semiconductor optical amplifier (SOA)], a modulator section, and a bandwidth-limiting optical filter. The laser is loss-modulated and the peak loss in the modulator section is zero. The laser is assumed to be mode-locked at the Nth harmonic, and therefore there are N optical pulses in the cavity. The cavity round-trip time is T_R, and the pulse repetition time is T_N, where $T_N = T_R/N$. The cavity round-trip frequency Ω_R and the pulse repetition frequency Ω_N are defined as $2\pi/T_R$ and $2\pi/T_N$, respectively. Below, we derive nonlinear discrete-time finite-difference equations to model the dynamics in harmonically mode-locked lasers. These equations are then linearized

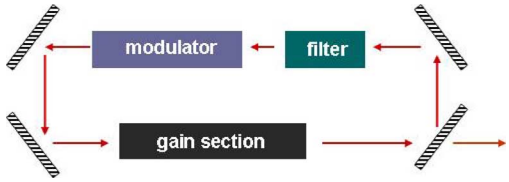

Fig. 2. Harmonically mode-locked semiconductor laser with a ring-shaped cavity.

to obtain finite-difference equations for the carrier and photon number fluctuations.

We assume that a pulse traveling inside the gain section is described by the complex amplitude $A(x,t)$, which is normalized such that $\int_{-\infty}^{\infty} |A(x,t)|^2\, dt$ equals the number of photons $n_p(x)$ in the pulse at location x in the gain section. In the gain section, the equation for the complex amplitude $A(x,t)$ (or the slowly varying envelope) of the pulse in the moving frame of reference is as follows [15]:

$$\frac{\partial A(x,t)}{\partial x} = j\frac{D}{2}\frac{\partial^2 A(x,t)}{\partial t^2} + \frac{g(x,t)}{2}(1-j\alpha)\,A(x,t) \quad (1)$$

where D is the modal dispersion (in s^2-cm^{-1}), $g(x,t)$ is the modal gain per unit length (incm^{-1}), and α is the semiconductor linewidth enhancement factor that describes the changes in the material refractive index that accompany changes in the material gain [16]. Effects due to finite gain bandwidth are ignored in (1) since it is assumed that the pulse bandwidth is limited by the optical filter in the cavity. The gain is assumed to depend linearly on the carrier density in the gain section

$$g(x,t) = \kappa\, n(x,t) \quad (2)$$

where $n(x,t)$ is the carrier density (in cm^{-1}) above the transparency carrier density $n_{\rm tr}$[16], and κ is the ratio of the differential gain of the material (in cm^2) and the effective area of the optical mode in the gain section [16]. The saturation pulse energy $E_{\rm sat}$ for the gain medium equals $\hbar\omega_o/\kappa$, where $\hbar\omega_o$ is the photon energy. In the presence of an optical pulse the carrier density satisfies the equation

$$\frac{dn(x,t)}{dt} = \frac{I_o}{q\,l_g} - \frac{n_{\rm tr}}{\tau_r} - \frac{n(x,t)}{\tau_r} - \kappa\, n(x,t)\,|A(x,t)|^2 \quad (3)$$

where I_o is the current pumped into the active region, q is the electric charge, l_g is the length of the gain section, and τ_r is the carrier recombination lifetime. We define a quantity n_c^- that is given by the relation

$$n_c^- = \int_0^{l_g} dx\, n(x, t_x^-). \quad (4)$$

Here, t_x^- is the time just before the pulse reaches the location x inside the gains section. n_c^- is therefore the total integrated carrier number in the gain section just before the pulse. Using the above differential equations that describe pulse propagation and amplification inside the gain section, one can derive the following exact relation for the pulse photon number before (n_p^-) and after (n_p^+) the gain section (see Appendix A):

$$n_p^+ = \frac{1}{\kappa}\log\left\{\exp\left(\kappa\, n_c^-\right)\left[\exp\left(\kappa\, n_p^-\right) - 1\right] + 1\right\}. \quad (5)$$

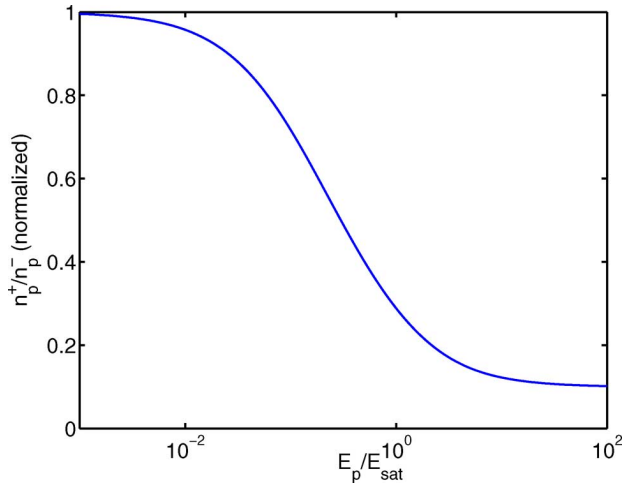

Fig. 3. Amplifier gain n_p^+/n_p^-, normalized to the unsaturated gain (assumed to be 10 dB) is plotted as a function of the normalized input pulse energy $E_p/E_{\rm sat}$.

The effect of dynamic gain saturation is shown in Fig. 3, which plots the gain n_p^+/n_p^- of the amplifier, normalized to the unsaturated gain, as a function of the normalized input pulse energy $E_p/E_{\rm sat}$. Pulses with larger energy see less gain than pulses with smaller energy. One can also define the total carrier number n_c^+ just after the pulse in the gain section by the relation

$$n_c^+ = \int_0^{l_g} dx\, n(x, t_x^+) \tag{6}$$

where t_x^+ is the time just after the pulse at location x. Assuming the pulse width to be short enough so that there is no significant carrier recombination taking place within the duration of the pulse, the increase in the pulse photon number must equal the decrease in the carrier number. Therefore

$$n_c^- - n_c^+ = n_p^+ - n_p^-. \tag{7}$$

Using (5) and (7), we can write finite-difference equations for the pulse photon number and the carrier number. Assuming that the net photon loss in the modulator section, the filter section, and from the output coupler can all be expressed by the multiplicative factor e^{-L} (see Appendix C), one can write the following equation relating the photon number $n_p[n+N]$ of the $(n+N)$th pulse just before entering the gain section to that of the nth pulse:

$$n_p[n+N] = \frac{1}{\kappa}\log\Big[\exp(\kappa\, n_c[n])\big[\exp(\kappa n_p[n]) - 1\big] + 1\Big]\exp(-L). \tag{8}$$

Here, $n_c[n]$ is the carrier number before the nth pulse. Note that $n_p[n+N]$ appears on the left-hand side of the above equation and not $n_p[n+1]$. This is because there are N pulses in the cavity and the nth pulse after one complete round trip becomes the $(n+N)$th pulse. Equation (8) represents N separate finite-difference equations for the N different pulses in the laser cavity. The carrier number $n_c[n+1]$ before the $(n+1)$th pulse can be obtained from $n_c[n]$ by using (3) and (7) to yield

$$\begin{aligned} n_c[n+1] &= \left\{ n_c[n] - \frac{1}{\kappa}\log\Big[\exp(\kappa\, n_c[n])\big[\exp(\kappa\, n_p[n]) - 1\big] + 1\Big] + n_p[n] \right\} \exp\left(\frac{-T_N}{\tau_r}\right) \\ &\quad + \left[\frac{I_o\,\tau_r}{q} - n_{\rm tr}\right]\left[1 - \exp\left(\frac{-T_N}{\tau_r}\right)\right]. \end{aligned} \tag{9}$$

Equations (8) and (9) constitute a system of $(N+1)$ nonlinear coupled finite-difference equations for the carrier number in the gain section and the number of photons in the N different pulses. These equations assume no coupling between the pulse photon number fluctuations and other pulse fluctuations. For example, in [13], it was shown that the pulse photon number fluctuations can couple to the pulse timing fluctuations in the presence of dynamic gain saturation. In this paper, we ignore such couplings for the sake of simplicity and because their inclusion have been found to not affect the main results presented in this paper in any significant way. These nonlinear equations can give more than one steady-state solution. The most desirable steady-state solution is the one in which all of the pulses are identical and there are no pulse dropouts. We assume a solution in which all of the pulses in the cavity have $n_{\rm po}$ number of photons just before entering the gain section, and the carrier number in the gain section just before each pulse is $n_{\rm co}$. These steady-state values satisfy

$$\kappa n_{\rm po}\exp(L) = \log\Big[\exp(\kappa\, n_{\rm co})\big[\exp(\kappa\, n_{\rm po}) - 1\big] + 1\Big] \tag{10}$$

and (11), shown at the bottom of the page. The stability of the assumed solution can be studied by linearizing the nonlinear equations in (9) and (8) around the steady state to obtain the following finite-difference equations for the pulse photon number and carrier number fluctuations, $\Delta n_p[n]$ and $\Delta n_c[n]$, respectively:

$$\Delta n_c[n+1] - \Delta n_c[n] = -\Delta n_c[n]\,\gamma_{cc} - \Delta n_p[n]\,\gamma_{cp} \tag{12}$$

$$\Delta n_p[n+N] - \Delta n_p[n] = -\Delta n_p[n]\,\gamma_{pp} + \Delta n_c[n]\,\gamma_{pc} \tag{13}$$

where γ_{cc} describes the decay of the carrier number fluctuation due to carrier recombination and stimulated emission, γ_{cp} describes the carrier number fluctuations induced by the photon number fluctuations, γ_{pp} describes the decay of the photon number fluctuations due to dynamic gain saturation, and

$$n_{\rm co}\left[1 - \exp\left(\frac{-T_N}{\tau_r}\right)\right] + n_{\rm po}\Big[\exp(L) - 1\Big]\exp\left(\frac{-T_N}{\tau_r}\right) = \left[\frac{I_o\,\tau_r}{q} - n_{\rm tr}\right]\left[1 - \exp\left(\frac{-T_N}{\tau_r}\right)\right]. \tag{11}$$

γ_{pc} describes the photon number fluctuations induced by the fluctuations in the carrier number. Equations (12) and (13) are a system of $(N+1)$ linear coupled finite-difference equations for the carrier and photon number fluctuations. Expressions for γ_{cc}, γ_{cp}, γ_{pp}, and γ_{pc} in (12) and (13) are given as follows:

$$\gamma_{cc}=1-\frac{\exp\left(\frac{-T_N}{\tau_r}\right)}{\exp(\kappa n_{co})\left[\exp(\kappa n_{po})-1\right]+1} \quad (14)$$

$$\gamma_{cp}=\frac{\left[\exp(\kappa n_{co})-1\right]\exp\left(\frac{-T_N}{\tau_r}\right)}{\exp(\kappa n_{co})\left[\exp(\kappa n_{po})-1\right]+1} \quad (15)$$

$$\gamma_{pp}=1-\exp\left(\frac{-T_N}{\tau_r}\right)\frac{\exp(\kappa n_{co})\exp(\kappa n_{po})}{\exp(\kappa n_{co})\left[\exp(\kappa n_{po})-1\right]+1} \quad (16)$$

$$\gamma_{pc}=\exp(-L)\frac{\exp(\kappa n_{co})\exp(\kappa n_{po})}{\exp(\kappa n_{co})\left[\exp(\kappa n_{po})-1\right]+1}. \quad (17)$$

The values of the parameters γ_{cc}, γ_{pp}, γ_{cp}, and γ_{pc} given above are for the specific model assumed here. The finite-difference equations in (12) and (13) are more general and can be used for most harmonically mode-locked lasers provided that the values of γ_{cc}, γ_{pp}, γ_{cp}, and γ_{pc} are available. In Section III, we determine the conditions necessary for the stability of this system.

III. Relaxation Oscillation Modes and Conditions for Stability

The system of finite-difference equations for the fluctuations in (12) and (13) can be solved by assuming a solution of the form

$$\Delta n_c[n]=n_c(z)\,z^n \quad (18)$$

$$\Delta n_p[n]=n_p(z)\,z^n. \quad (19)$$

Substituting (19) into (12) and (13), we find

$$n_c(z)=-\frac{\gamma_{cp}}{z-1+\gamma_{cc}}n_p(z) \quad (20)$$

and the allowed values of z are the complex roots of an $(N+1)$th order polynomial

$$z^{N+1}-z^N(1-\gamma_{cc})-z(1-\gamma_{pp}) +(1-\gamma_{cc})(1-\gamma_{pp})+\gamma_{cp}\gamma_{pc}=0. \quad (21)$$

The polynomial above has in $(N+1)$ complex roots z_m ($m=1,2,\ldots(N+1)$) which correspond to $(N+1)$ relaxation oscillation modes. The assumed steady-state solution is stable if and only if the magnitudes of all the roots are less than unity. The roots z_m determine the pattern of the photon number (or the energy) fluctuations in pulses inside the laser cavity corresponding to each relaxation oscillation mode. Since the polynomial in (21) has real coefficients, the complex roots come in complex conjugate pairs. The first conjugate pair of roots correspond to relaxation oscillation modes in which the photon number (or the energy) of different pulses inside the laser cavity fluctuate in phase. The higher order roots correspond to relaxation oscillation modes in which the photon number fluctuations of different pulses inside the laser cavity are increasingly out of phase. The general trends are best illustrated by an example.

TABLE I
Laser Parameter Values Used in Simulations (Unless Stated Otherwise)

Laser differential gain dg/dn	10^{-15} cm^2
Effective mode area A_{eff}	10^{-8} cm^2
κ $(=dg/dn/A_{eff})$	10^{-7}
Fundamental roundtrip time T_R	0.2 ns
Cavity loss e^{-L}	0.25
Carrier lifetime τ_r	0.8 ns
Transparency carrier density n_{tr}	1.6×10^{18} cm^{-3}

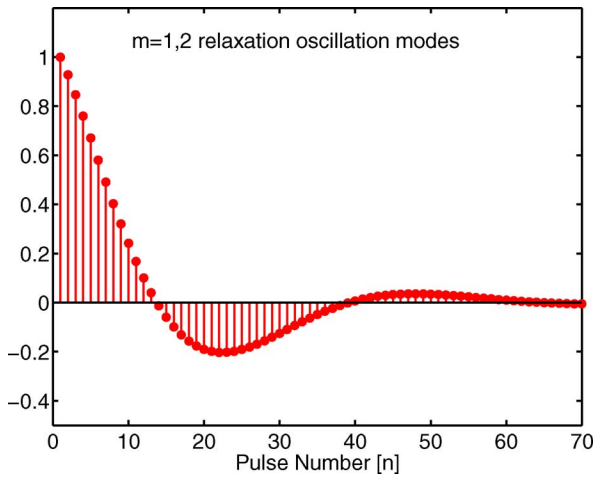

Fig. 4. Time evolution of the photon number fluctuations for the first and second ($m=1,2$) relaxation oscillation modes for an $N=6$ harmonically mode-locked laser.

The roots z_m can easily be obtained by numerically solving the equation in (21). For simulations, unless stated otherwise, we use the laser parameter values listed in Table I. Fig. 4 shows the time evolution of the pulse photon number fluctuations (normalized units) for the first two relaxation oscillation modes ($m=1$ and $m=2$) as a function of the pulse number for a $N=6$ harmonically mode-locked laser. It should be noted that every $(N+1)$th pulse is the same pulse after a cavity round trip. The pulse energy is $0.1\,E_{\rm sat}$. The photon number fluctuations in all of the pulses inside the laser cavity are seen to be in phase.

Fig. 5 shows the time evolution of the photon number fluctuations for the third and fourth relaxation oscillation modes ($m=3$ and $m=4$). Fig. 6 shows the photon number fluctuations corresponding to the fifth and sixth relaxation oscillation modes ($m=5$ and $m=6$). It can be seen that the photon number fluctuations among the pulses in the cavity are increasingly out of phase for higher order relaxation oscillation modes. Fig. 7 shows the photon number fluctuations for the highest ($m=7$) relaxation oscillation mode. For the highest mode, the energy fluctuations in the neighboring pulses inside the laser cavity are completely out of phase. Also, Figs. 4–7 show that the higher order relaxation oscillation modes are less damped than the lower order modes. In Section III-A, we analytically determine the conditions necessary for the stability of the relaxation oscillation modes.

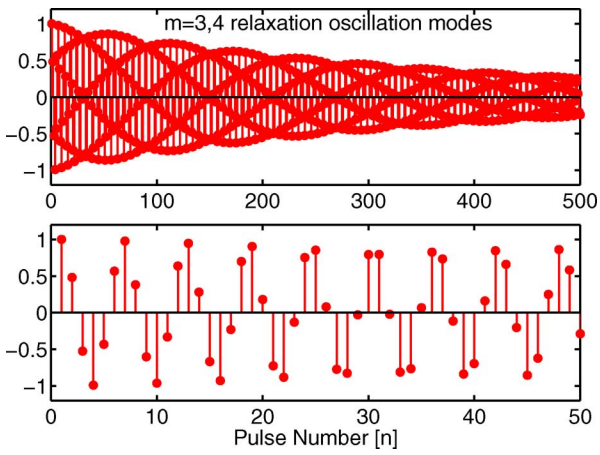

Fig. 5. Time evolution of the photon number fluctuations for the third and fourth ($m = 3, 4$) relaxation oscillation modes for a $N = 6$ harmonically mode-locked laser.

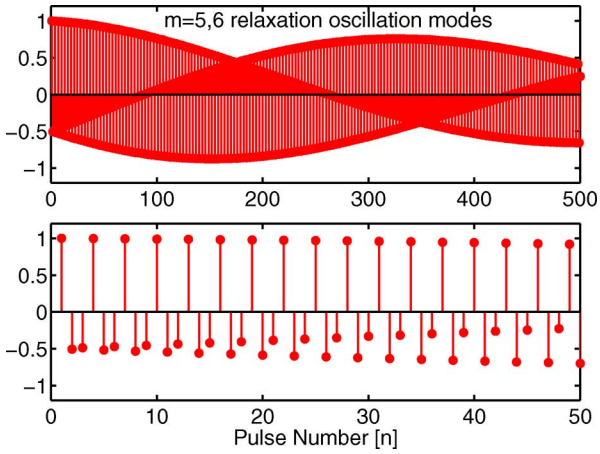

Fig. 6. Time evolution of the photon number fluctuations for the fifth and sixth ($m = 5, 6$) relaxation oscillation modes for a $N = 6$ harmonically mode-locked laser.

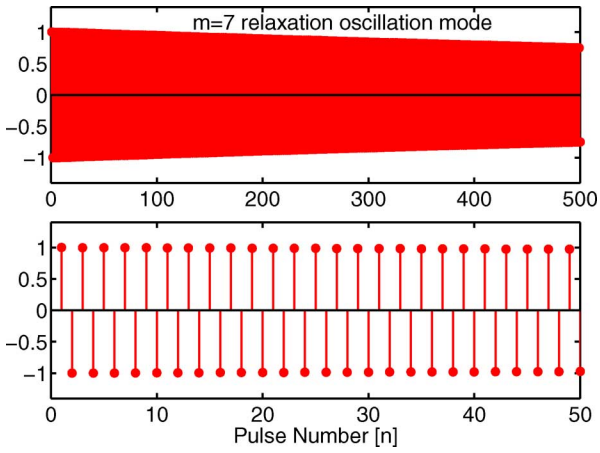

Fig. 7. Time evolution of the photon number fluctuations for the seventh ($m = 7$) relaxation oscillation mode for a $N = 6$ harmonically mode-locked laser.

A. Stability of Fundamentally Mode-Locked Operation

For fundamentally mode-locked operation ($N = 1$), the two roots of the second-order polynomial in (21) are complex conjugates of each other and have magnitude given by

$$|z_1| = |z_2| = \sqrt{1 - (\gamma_{cc} + \gamma_{pp} - \gamma_{cc}\gamma_{pp} - \gamma_{cp}\gamma_{pc})}. \quad (22)$$

Therefore, fundamentally mode-locked operation will be stable if (and only if) the following condition is satisfied:

$$\gamma_{cc} + \gamma_{pp} > \gamma_{cc}\gamma_{pp} + \gamma_{cp}\gamma_{pc}. \quad (23)$$

For γ_{cc}, γ_{pp}, γ_{cp}, and γ_{pc} given in (14)–(17), and using the relation in (10), it can be shown that (23) is satisfied for all pulse energies. Fundamentally mode-locked operation is therefore stable with respect to relaxation oscillations.

B. Stability of Harmonically Mode-Locked Operation

A complete analytical analysis of the stability of harmonically mode-locked operation is complicated. It can be shown that a necessary (but not sufficient) condition for all of the roots of the polynomial in (21) to have magnitude less than unity is (see Appendix B)

$$2\gamma_{pp} > \gamma_{cc}\gamma_{pp} + \gamma_{cp}\gamma_{pc}. \quad (24)$$

The above relation is the most important result of this paper, and it sets the limits for stable harmonic mode-locking in semiconductor lasers. The condition in (24) shows that harmonic mode-locking is not stable if $\gamma_{pp} = 0$. This result can be understood in a simple way. The slow response of the gain medium is tied to the total energy in all of the pulses in the laser cavity. Pulse energy fluctuations that are positively correlated in different pulses are damped by the slow negative feedback from the gain medium. These positively correlated pulse energy fluctuations correspond to the lower order relaxation oscillation modes. Pulse energy fluctuations that are negatively correlated in different pulses are not damped by the slow response of the gain medium. These negatively correlated pulse energy fluctuations correspond to the higher order relaxation oscillation modes. Therefore, dynamic gain saturation that results in a nonzero positive value for γ_{pp} helps to stabilize harmonic mode-locking in semiconductor lasers with respect to relaxation oscillations.

In [6] and [7] the stability of harmonically mode-locked fiber lasers was attributed to the soliton effect, and the stability condition derived there is equivalent to $\gamma_{pp} > 0$ in the language used in this paper (although γ_{pp} in [6] and [7] was entirely due to the soliton effect and not due to dynamic gain saturation). Slow gain dynamics were ignored in [6] and [7] since they were expected to play a minor role in fiber lasers. The condition in (24) sets a more stringent condition for stability since slow gain dynamics tend to destabilize harmonic mode-locking in semiconductor lasers.

The condition necessary for stability given in (24) can also be derived in a simple way by estimating the largest (in magnitude)

root z_{N+1} of the equation in (21). When N is even, z_{N+1} is real and is assumed to be given by the approximate expression

$$z_{N+1} \approx \exp\left(-\gamma_{N+1} + j\,\pi\right). \tag{25}$$

The assumed form in (25) is such that the pulse energy fluctuations in the $(N+1)$th relaxation oscillation mode are completely negatively correlated in the neighboring pulses. We substitute (25) into (21) and expand to first order in γ_{N+1} to obtain

$$\gamma_{N+1} \approx \frac{2\gamma_{pp} - \gamma_{cc}\,\gamma_{pp} - \gamma_{cp}\,\gamma_{pc}}{N\,(2-\gamma_{cc}) + \gamma_{pp}}. \tag{26}$$

The methods used to obtain (26) are justified as long as the magnitude of the resulting value of γ_{N+1} is much less than unity. The pulse energy fluctuations are stable if $\gamma_{N+1} > 0$. Equation (26) shows that $\gamma_{N+1} > 0$ provided the condition for stability given earlier in (24) is satisfied. Numerical simulations confirm that the approximate form for z_{N+1} assumed in (25) is accurate as long as $|\gamma_{N+1}| \ll 1$, which is almost always the case in semiconductor mode-locked lasers. For N odd, the solution in (25) is not a good approximation. $(z_{N+1})^{N+1}$ must have the same sign as z_{N+1}. This is because the $(N+1)$th pulse is the same pulse after one complete round trip. The noise in a pulse evolves slowly and is not expected to change sign in one round trip. Numerical simulations show that, for N odd, the largest (in magnitude) roots z_{N+1} and z_N of (21) are complex conjugates of each other and are given to a very good approximation by

$$\begin{aligned} z_{N+1} &\approx \exp\left[-\gamma_{N+1} + j\,\pi\left(1 - \frac{1}{N}\right)\right] \\ z_N &\approx \exp\left[-\gamma_N - j\,\pi\left(1 - \frac{1}{N}\right)\right]. \end{aligned} \tag{27}$$

The solution above represents the maximum possible negative correlation between the neighboring pulses when N is odd. The approximate value of γ_{N+1} is found as before as

$$\gamma_{N+1} \approx \frac{\gamma_{pp}\,\left(\exp\left(\frac{-j\,\pi}{N}\right)+1\right) - \left(\gamma_{cc}\,\gamma_{pp} + \gamma_{cp}\,\gamma_{pc}\right)}{N\,\left(\exp\left(\frac{-j\,\pi}{N}\right)+1-\gamma_{cc}\right) + \gamma_{pp}\exp\left(\frac{-j\,\pi}{N}\right)} \tag{28}$$

where γ_N is just the complex conjugate of γ_{N+1}. For N odd, γ_{N+1} and γ_N are in general complex, and pulse energy fluctuations are stable if $\mathrm{Re}\left(\gamma_{N+1}\right) = \mathrm{Re}\left(\gamma_N\right) > 0$, which is the case if the condition for stability given in (24) is satisfied.

C. Damping of the Relaxation Oscillation Modes

In general, the difference $1 - |z_m|$ is proportional to the damping of the mth relaxation oscillation mode. A negative value of $1 - |z_m|$ would imply instability. Since the highest order relaxation oscillation mode is the least damped, $1 - |z_{N+1}|$ determines the stability of the laser (note that $\mathrm{Re}\left(\gamma_{N+1}\right) \approx 1 - |z_{N+1}|$). The larger the value of $1 - |z_{N+1}|$, the stronger the damping of the highest relaxation oscillation mode, and the more stable will be the laser against noise and pulse dropouts. In case of the model presented in this paper, the value of $1 - |z_{N+1}|$ depends on the ratio of the pulse energy E_p to the saturation pulse energy E_{sat} of the gain medium defined earlier, the ratio of the pulse repetition time T_N to the carrier recombination time τ_r, and the cavity round-trip loss e^{-L}. Fig. 8 shows the value of $1 - |z_{N+1}|$ as a function of the ratio E_p/E_{sat} for a $N = 20$ harmonically mode-locked laser with a cavity round-trip time T_R equal to 2 ns. The different curves correspond to different values of the cavity round-trip loss e^{-L}. All other laser parameters are as in Table I. A larger pulse energy causes more dynamic gain saturation, resulting in increased damping and better pulse stability for harmonically mode-locked operation. Fig. 8 shows that dynamic gain saturation ensures that harmonic mode-locking is stable against relaxation oscillations even for very small pulse energies. It needs to be pointed out here that, at very small pulse energies, the damping of the relaxation oscillations can become weak, and the noise-induced pulse fluctuations can become large, such that the linearized analysis presented in this paper may no longer be valid. Fig. 9 shows the value of $1 - |z_{N+1}|$ as a function of the ratio E_p/E_{sat} for different values of N. The assumed values of e^{-L} and T_R are 0.4 and 2 ns, respectively. A smaller value of N implies a longer pulse repetition interval, larger damping of the carrier number fluctuations from pulse to pulse, and therefore better stability for harmonic mode-locking against gain dynamics at slow time scales.

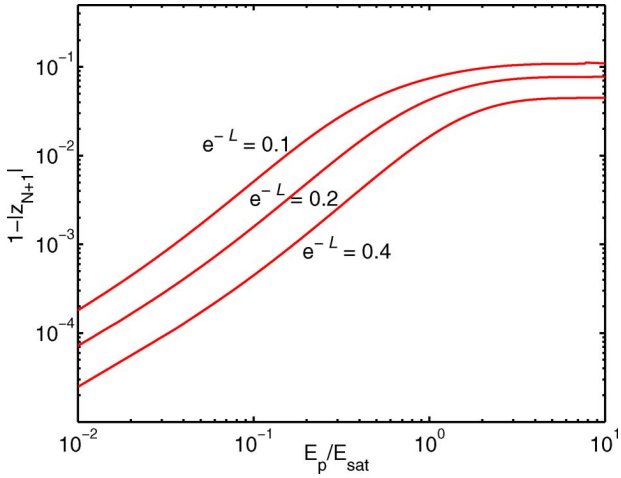

Fig. 8. $1 - |z_{N+1}|$ is plotted as a function of E_p/E_{sat} for different values of the cavity round-trip loss e^{-L} for a $N = 20$ harmonically mode-locked laser with a cavity round-trip time T_R equal to 2 ns.

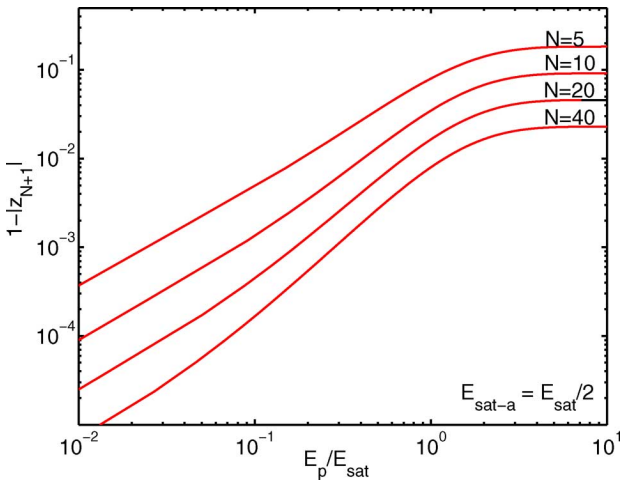

Fig. 9. $1 - |z_{N+1}|$ is plotted as a function of E_p/E_{sat} for different values of N. The assumed values of e^{-L} and T_R are 0.4 and 2 ns, respectively.

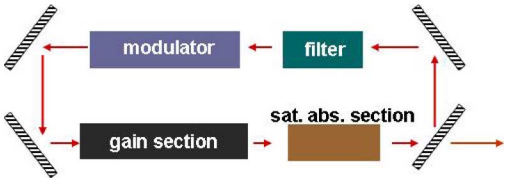

Fig. 10. Harmonically mode-locked semiconductor laser with a saturable absorber section.

IV. Effect of Saturable Absorber on Harmonic Mode-Locking in Semiconductor Lasers

So far, we have considered a mode-locked laser without a saturable absorber section. A saturable absorber helps generate shorter pulses. In many practical cases, saturable absorption is present in a semiconductor amplifier even when a separate section is not explicitly included due to light absorption at defect sites or in unpumped regions of the optical waveguide. A saturable absorber can destabilize harmonic mode-locking since it offers less loss to larger energy pulses compared with smaller energy pulses, and this can make the higher order relaxation oscillation modes unstable. We consider the laser cavity shown in Fig. 10, in which a saturable absorber is added after the gain section.

We assume that the saturable absorber is slow (i.e., the loss recovers on a time scale much longer than the pulse width) but the loss recovers on a time scale much shorter than the pulse repetition interval (so that slow loss dynamics can be neglected). The total unsaturated loss of the absorber is given by the multiplicative factor e^{-L_a}. The saturation pulse energy for the absorber is given by the expression

$$E_{\mathrm{sat-a}} = \frac{\hbar\omega_o}{\kappa_a} \tag{29}$$

where κ_a is the ratio of the differential loss of the material (in cm^2) and the effective area of the optical mode in the absorber section [16]. For pulse shaping with a slow saturable absorber, one must have the saturation energy E_{sat} of the gain section larger than $E_{\mathrm{sat-a}}$ [17]. We assume in this paper that $E_{\mathrm{sat-a}} = E_{\mathrm{sat}}/2$. One can derive the following nonlinear finite-difference equation for the pulse photon numbers and the carrier number in the gain section using the methods described earlier:

$$n_{pa}[n] = \frac{1}{\kappa}\log\left[\exp(\kappa\, n_c[n])\left[\exp\left(\kappa n_p[n]\right) - 1\right] + 1\right] \tag{30}$$

$$n_p[n+N] = \frac{1}{\kappa_a}\log\left[\exp\left(-L_a\right)\left[\exp\left(\kappa_a\, n_{pa}[n]\right) - 1\right] + 1\right] \times \exp\left(-L\right) \tag{31}$$

$$n_c[n+1] = \left\{n_c[n] - n_{pa}[n] + n_p[n]\right\}\exp\left(\frac{-T_N}{\tau_r}\right) + \left[\frac{I_o\,\tau_r}{q} - n_{tr}\right]\left[1 - \exp\left(\frac{-T_N}{\tau_r}\right)\right]. \tag{32}$$

Here, $n_{pa}[n]$ is an extra variable that stands for the photon number of the nth pulse just before entering the saturable absorber section. The above equations include gain dynamics on both fast and slow time scales and loss dynamics on just the fast time scales. Therefore, dynamic loss saturation, which tends to destabilize harmonic mode-locking, is included in the model. Assuming a steady state in which the energies of all pulses in the cavity are the same, the above equations can be linearized to obtain finite-difference equations for the pulse photon number fluctuations and the carrier number fluctuations. These linearized equations are identical in form to the equations given earlier in (12) and (13) except that the expressions for the parameters γ_{pp} and γ_{pc} are different and are given in Appendix D.

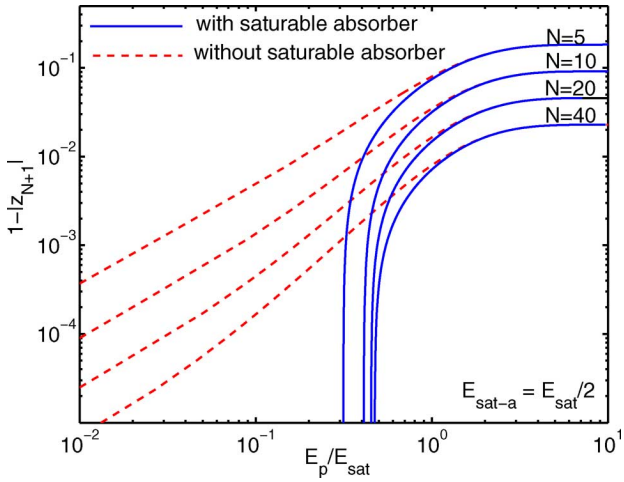

Fig. 11. $1-|z_{N+1}|$ is plotted as a function of E_p/E_{sat} for different values of N for a harmonically mode-locked laser both with (solid) and without (dashed) a saturable absorber. The assumed values of e^{-L}, e^{-L_a}, and T_R are 0.4, 0.6, and 2 ns, respectively. Harmonic mode-locking becomes unstable for pulse energies much smaller than E_{sat} in the presence of a saturable absorber.

The stability of harmonic mode-locking with respect to relaxation oscillations in the presence of the saturable absorber can be studied by looking the at value of the damping factor $1-|z_{N+1}|$ corresponding to the highest relaxation oscillation mode. Recall that stability demands $1-|z_{N+1}| > 0$. Fig. 11 plots $1-|z_{N+1}|$ as a function of the ratio E_p/E_{sat} for different values of N for a harmonically mode-locked laser both with and without a saturable absorber. The assumed values of e^{-L}, e^{-L_a}, and T_R are 0.4, 0.6, and 2 ns, respectively, and $E_{\mathrm{sat-a}} = E_{\mathrm{sat}}/2$. The vertical slopes of the curves for the saturable absorber case correspond to the values of $1-|z_{N+1}|$ becoming negative below certain minimum pulse energies and indicate the range of stability with respect to relaxation oscillations. For pulse energies much smaller than the gain saturation energy E_{sat}, dynamic gain saturation is not able to stabilize harmonic mode-locking in the presence of dynamic loss saturation. For large pulse energies, both the gain and the loss are saturated, and harmonic mode-locking is stable.

It was pointed out earlier that lower order relaxation modes are more stable and/or more strongly damped than higher order modes. Fig. 12 plots $1-|z_m|$ as a function of the ratio E_p/E_{sat} for different values of m for a $N = 10$ harmonically mode-locked laser. The assumed values of e^{-L}, e^{-L_a}, and T_R are 0.4, 0.6, and 2 ns, respectively, and $E_{\mathrm{sat-a}} = E_{\mathrm{sat}}/2$. It can be seen that modes 1–4 are stable even for small pulse energies while modes 5–11 become unstable for small pulse energies. The higher stability of lower order relaxation oscillation modes is evident from the figure.

The range of stability depends on the strength of the saturable absorber (measured in terms of the total unsaturated loss). Fig. 13 plots the value of $1-|z_{N+1}|$ as a function of the ratio

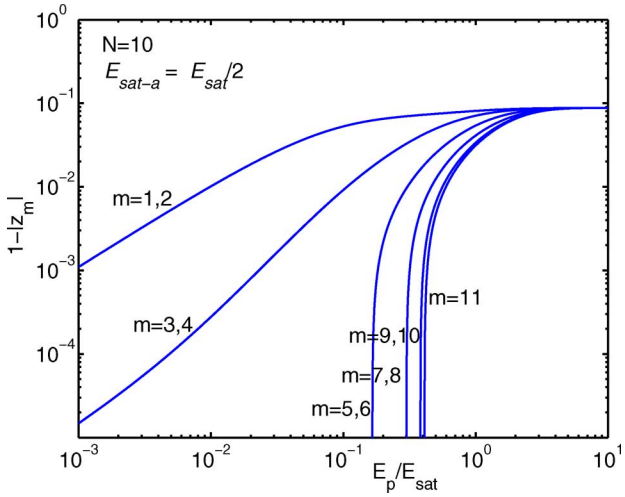

Fig. 12. $1-|z_m|$ is plotted as a function of $E_p/E_{\rm sat}$ for different values of m for an $N=10$ harmonically mode-locked laser with a saturable absorber. The assumed values of e^{-L}, e^{-L_a}, and T_R are 0.4, 0.6, and 2 ns, respectively, and $E_{\rm sat-a}=E_{\rm sat}/2$. Modes 1–4 are stable even for small pulse energies while modes 5–11 become unstable for small pulse energies.

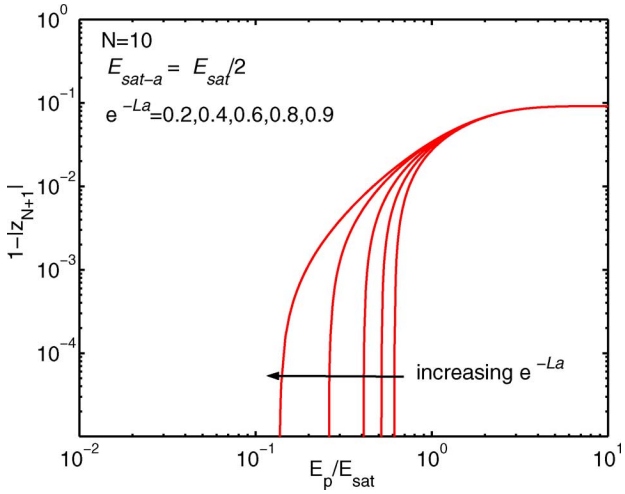

Fig. 13. $1-|z_{N+1}|$ is plotted as a function of $E_p/E_{\rm sat}$ for different values of the unsaturated loss e^{-L_a} in the absorber for an $N=10$ harmonically mode-locked laser with a saturable absorber. The assumed values of e^{-L} and T_R are 0.4 and 2 ns, respectively, and $E_{\rm sat-a}=E_{\rm sat}/2$. Harmonic mode-locking is stable for smaller pulse energies when the saturable absorber is weak.

$E_p/E_{\rm sat}$ for different values of the unsaturated loss e^{-L_a} in the absorber for a $N=10$ harmonically mode-locked laser. The assumed values of e^{-L} and T_R are 0.4 and 2 ns, respectively, and $E_{\rm sat-a}=E_{\rm sat}/2$. Harmonic mode-locking is stable for smaller pulse energies when the saturable absorber is weaker.

A fast saturable absorber, instead of a slow saturable absorber, would change the analysis presented above, but the final form of the linearized equations would still come out to be the same as the equations given in (12) and (13). The values of γ_{pp} and γ_{pc} would be different than the values given in Appendix D, but the basic features and trends in the results presented above for the slow saturable absorber case are expected to remain unchanged.

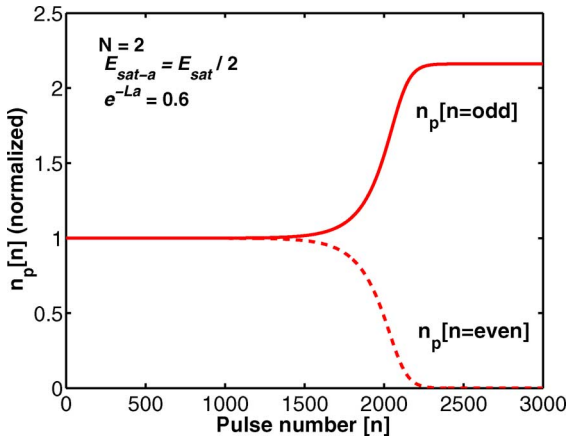

Fig. 14. Time-dependent photon numbers (normalized to the initial photon number) of the two pulses in a $N=2$ harmonically mode-locked laser (with a saturable absorber) are plotted as a function of time. The assumed values of e^{-L}, e^{La}, and T_R are 0.4, 0.6, and 2 ns, respectively, and $E_{\rm sat-a}=E_{\rm sat}/2$. Harmonic mode-locking is unstable for the small initial pulse energies and leads to one pulse dropping out.

V. Pulse Dropouts

Any initial noise-induced perturbation can always be expanded in terms of the relaxation oscillation modes, and the most general solution for $\Delta n_c[n]$ and $\Delta n_p[n]$ can be written as

$$\Delta n_c[n]=\sum_{m=1}^{N+1} n_c(z_m)\, z_m^n \tag{33}$$

$$\Delta n_p[n]=\sum_{m=1}^{N+1} n_p(z_m)\, z_m^n \tag{34}$$

where z_m represents the roots of the polynomial in (21). If an unstable relaxation oscillation mode is excited, then the energies of certain pulses will grow with time, while the energies of other pulses will decrease with time, depending on the pattern of the photon number fluctuations corresponding to that mode. This can lead to pulse dropouts. As an example, we consider an $N=2$ harmonically mode-locked laser with a saturable absorber. The assumed values of e^{-L}, e^{-L_a}, and T_R are 0.4, 0.6, and 2 ns, respectively, and $E_{\rm sat-a}=E_{\rm sat}/2$. We start by assuming an operating point that is a solution of the time-independent version of the nonlinear finite-difference equations given in (30)–(32). The initial energies of both the pulses inside the cavity were the same and equal to $\sim 0.15\ E_{\rm sat}$. For these pulse energies, the linearized analysis discussed above gives $z_3=-1.0072$. The magnitude of z_3 is greater than unity, and therefore the assumed operating point is unstable with respect to fluctuations that are negatively correlated in the two pulses inside the cavity. The magnitudes of z_1 and z_2 are less than unity. The results obtained by simulating the nonlinear finite-difference equations given in (30)–(32) in time are shown in Fig. 14, which plots the photon number of both the pulses inside the laser cavity as a function of time. During the simulation, numerical errors produced a perturbation in which photon number fluctuations were negatively correlated in the two pulses. The fluctuations grew in time until one pulse completely dropped out and, in steady state, only one pulse existed in the cavity. It is favorable for one pulse to become more energetic at the expense of

the other pulse and thereby reduce losses in the saturable absorber. This simulation shows that instabilities observed in the linearized analysis can lead to pulse dropouts.

VI. Conclusion

In this paper, we have presented conditions necessary for the stability of harmonically mode-locked semiconductor lasers with respect to relaxation oscillations. Relaxation oscillation modes in harmonically mode-locked lasers can have pulse energy fluctuations that are negatively correlated among different pulses inside the laser cavity, and these modes can cause instability. We have shown that dynamic gain saturation can stabilize harmonic mode-locking. In the presence of a saturable absorber, stable operation is obtained only for pulse energies above a minimum value. The model presented in this paper has ignored nonlinear effects, such as Kerr nonlinearity and two-photon absorption, that could become important for high-intensity pulses and affect pulse stability in harmonically mode-locked lasers.

The predictions in this paper can be verified experimentally. For example, in [12], it was shown that the spectral weights of the supermode noise peaks in the experimentally measured pulse noise spectral density functions can be related to the correlations in the noise of different pulses inside the laser cavity. Negatively correlated pulse energy fluctuations correspond to increased spectral weight in the supermode noise peaks located near the odd integral multiples of one-half the pulse repetition frequency. Therefore, relaxation oscillation induced instability should manifest itself in the experimentally measured spectral weights of the supermode noise peaks.

Appendix A
Nonlinear Equation for the Pulse Photon Number

We start from (3) that

$$\frac{dn(x,t)}{dt} = \frac{I_o}{q\,l_g} - \frac{n_{tr}}{\tau_r} - \frac{n(x,t)}{\tau_r} - \kappa\, n(x,t)\,|A(x,t)|^2. \quad (35)$$

Within the duration of the pulse, and assuming the duration of the pulse to be much shorter than the carrier relaxation time τ_r), the above equation becomes

$$\frac{dn(x,t)}{dt} = -\kappa\, n(x,t)\,|A(x,t)|^2. \quad (36)$$

Integrating the above equation, we obtain the time-dependent gain $g(x,t)$ seen by the pulse

$$g(x,t) = \kappa\, n(x,t_x^-)\,\exp\left(-\kappa \int_{t_x^-}^{t} dt'\,|A(x,t')|^2\right) \quad (37)$$

where t_x^- is a time just before the pulse reaches the location x in the gain section. The equation for the pulse photon number is obtained by substituting (37) into (1), multiplying both sides by $A^*(x,t)$, integrating over the time variable t, and keeping the real part of the resulting equation. This yields

$$\frac{\partial n_p(x)}{\partial x} = n(x,t_x^-)\,\left[1-\exp\left(-\kappa\, n_p(x)\right)\right]. \quad (38)$$

Equation (38) can be integrated to give a relation between the pulse photon numbers n_p^- and n_p^+ at the input and output of the gain section, respectively, as

$$n_p^+ = \frac{1}{\kappa}\log\left\{\exp\left(\kappa\, n_c^-\right)\left[\exp\left(\kappa\, n_p^-\right)-1\right]+1\right\} \quad (39)$$

where n_c^- is defined by

$$n_c^- = \int_0^{l_g} dx\, n(x,t_x^-). \quad (40)$$

Appendix B
Necessary Condition for the Stability of Harmonically Mode-Locked Operation

Stability of harmonic mode-locking requires that the magnitude of all the roots of the following equation are less than unity:

$$z^{N+1} - z^N(1-\gamma_{cc}) - z(1-\gamma_{pp}) + (1-\gamma_{cc})(1-\gamma_{pp}) + \gamma_{cp}\,\gamma_{pc} = 0. \quad (41)$$

We use a bilinear transformation from the complex z-plane into the s-plane that maps the region inside the unit circle (i.e., $|z| < 1$) into the left half plane (i.e., $\mathrm{Re}(s) < 0$) to yield

$$z = \frac{1+s}{1-s} \quad \Longleftrightarrow \quad s = \frac{z-1}{z+1}. \quad (42)$$

The roots z_k will have magnitude less than unity if all solutions of the equation below are in the left half plane (i.e., have negative real parts) as

$$\left(\frac{1+s}{1-s}\right)^{N+1} - \left(\frac{1+s}{1-s}\right)^{N}(1-\gamma_{cc}) - \left(\frac{1+s}{1-s}\right)(1-\gamma_{pp}) + (1-\gamma_{cc})(1-\gamma_{pp}) + \gamma_{cp}\,\gamma_{pc} = 0. \quad (43)$$

After multiplying by $(1-s)^{N+1}$ in (43), we obtain an equation of the form

$$\sum_{k=0}^{N+1} a_k\, s^k = 0. \quad (44)$$

The coefficients a_k can be obtained from (43). The necessary (but not sufficient) conditions for the roots of (44) to have negative real parts are as follows.

1) All of the $(N+2)$ coefficients a_k must have the same sign.
2) All a_k must be nonzero, unless a_k for all even k or all odd k are zero.

The above two conditions give the necessary condition for the stability of harmonic mode-locking given in (24). For the $N=1$ fundamentally mode-locked case, the above conditions are also sufficient. For $N > 1$, the well-known Routh–Hurwitz criteria

can be used to analyze the necessary as well as sufficient conditions for the roots of (44) to have negative real parts [18].

APPENDIX C
MODELING MODULATOR, FILTER, AND OUTPUT COUPLING LOSSES

Modulator Section Loss: Pulse propagation in the modulator section is described by the equation [15]

$$\frac{\partial A(x,t)}{\partial x} = \frac{\alpha_m}{2}\left\{\cos\left[\Omega_N\left(t+\frac{x}{v_g}\right)\right]-1\right\}A(x,t) \quad (45)$$

$$\approx -\frac{\alpha_m}{4}\Omega_N^2 t^2 A(x,t) \quad (46)$$

where α_m is the loss per unit length (in cm^{-1}) and v_g is the group velocity of the pulse. The approximation in (46) is valid if the pulse transit time through the modulator is much smaller than the pulse width. The above equation can be integrated to obtain a relation between the number of photons in the pulse at the input and output of the modulator

$$n_p(\text{out}) = n_p(\text{in})\,(1-L_m) \approx n_p(\text{in})\,\exp(-L_m) \quad (47)$$

where the modulator loss L_m is

$$L_m = \frac{\alpha_m\, l_m}{2}\,\Omega_N^2\,\tau^2\,\frac{\int_{-\infty}^{\infty} dy\, y^2 |A(x,y\tau)|^2}{\int_{-\infty}^{\infty} dy\,|A(x,y\tau)|^2}. \quad (48)$$

Here, l_m is the length of the modulator section, and τ is the pulse width. The variable y in $A(x,y\tau)$ indicates the pulse shape at the location of the modulator.

Optical Filter Loss: We assume that the transmitivity $T(\omega)$ through the optical filter near the frequency ω_o of peak transmission is given by the equation

$$T(\omega) = 1 - \frac{(\omega-\omega_o)^2}{\omega_B^2} \quad (49)$$

where ω_B is the bandwidth of the filter. ω_o is also assumed to be equal to the pulse center frequency. The photon loss in the optical filter is then given by the relation [15]

$$n_p(\text{out}) = n_p(\text{in})\,(1-L_f) \approx n_p(\text{in})\,\exp(-L_f) \quad (50)$$

where the filter loss L_f is

$$L_f = \frac{1}{\omega_B^2\,\tau^2}\,\frac{\int_{-\infty}^{\infty} dy \left|\frac{\partial A(x,y\tau)}{\partial y}\right|^2}{\int_{-\infty}^{\infty} dy\,|A(x,y\tau)|^2}. \quad (51)$$

The variable y in $A(x,y\tau)$ indicates the pulse shape at the location of the filter.

Output Coupling Loss: The photon loss in the cavity from the output coupler and from the insertion losses associated with various components is given by the exponential function $\exp(-L_c)$. For example, if the reflectivity of the output coupler is R, then the contribution of the output coupler to L_c is $\log(1/R)$.

Total Loss: If the total round-trip loss is described by the multiplicative factor e^{-L} then L equals

$$L = L_c + L_m + L_f \quad (52)$$

where the expressions for L_c, L_m, and L_f were given in the previous sections. In most cases, $L_c \gg L_m, L_f$.

APPENDIX D
EXPRESSIONS FOR γ_{cc}, γ_{cp}, γ_{pp}, AND γ_{pc} IN THE PRESENCE OF THE SATURABLE ABSORBER

The expressions are as follows:

$$\gamma_{cc} = 1 - \frac{\exp\left(-\frac{T_N}{\tau_r}\right)}{\exp(\kappa\, n_{co})\left[\exp(\kappa\, n_{po})-1\right]+1} \quad (53)$$

$$\gamma_{cp} = \frac{\left[\exp(\kappa\, n_{co})-1\right]\exp\left(-\frac{T_N}{\tau_r}\right)}{\exp(\kappa\, n_{co})\left[\exp(\kappa\, n_{po})-1\right]+1} \quad (54)$$

$$\gamma_{pp} = 1 - \frac{\exp(-L_a)\exp(\kappa_a\, n_{pao})}{\exp(-L_a)\left[\exp(\kappa_a\, n_{pao})-1\right]+1} \cdot \exp\left(-\frac{T_N}{\tau_r}\right)\frac{\exp(\kappa\, n_{co})\exp(\kappa\, n_{po})}{\exp(\kappa n_{co})\left[\exp(\kappa\, n_{po})-1\right]+1} \quad (55)$$

$$\gamma_{pc} = \frac{\exp(-L_a)\exp(\kappa_a\, n_{pao})}{\exp(-L_a)\left[\exp(\kappa_a\, n_{pao})-1\right]+1} \cdot \exp(-L)\frac{\exp(\kappa\, n_{co})\exp(\kappa\, n_{po})}{\exp(\kappa n_{co})\left[\exp(\kappa\, n_{po})-1\right]+1}. \quad (56)$$

ACKNOWLEDGMENT

The authors would like to thank Dr. F. Bartoli for support through the National Science Foundation Faculty CAREER Award.

REFERENCES

[1] T. G. Ulmer, M. C. Gross, K. M. Patel, J. T. Simmons, and P. W. Juodawlkis, "160-Gb/s optically time-division multiplexed link with all-optical demultiplexing," *J. Lightw. Technol.*, vol. 18, no. 12, pp. 1964–1977, Dec. 2000.

[2] P. W. Juodawlkis, J. C. Twichell, G. E. Betts, J. J. Hargreaves, R. D. Younger, J. L. Wasserman, F. J. O'Donnell, K. G. Ray, and R. C. Williamson, "Optically sampled analog-to-digital converters," *IEEE Trans. Microw. Theory Tech.*, vol. 49, no. 10, pt. 2, pp. 1840–1853, Oct. 2001.

[3] C. M. DePriest, A. Braun, J. H. Abeles, E. Park, and P. Delfyett Jr., "10-GHz ultralow-noise optical sampling stream from a semiconductor diode ring laser," *IEEE Photon. Technol. Lett.*, vol. 13, no. 11, pp. 1109–1111, Nov. 2001.

[4] M. Horowitz, C. R. Menyuk, T. F. Carruthers, and I. N. Duling, "Theoretical and experimental study of harmonically modelocked fiber lasers for optical communication systems," *J. Lightw. Technol.*, vol. 18, no. 11, pp. 1565–1574, Nov. 2000.

[5] M. Nakazawa, E. Yoshida, and Y. Kimura, "Ultrastable harmonically and regeneratively modelocked polarisation-maintaining erbium fibre ring laser," *Electron. Lett.*, vol. 30, pp. 1603–1605, 1994.

[6] H. A. Haus, "Long term storage of a bit stream of solitons," *Opt. Lett.*, vol. 17, pp. 1500–1502, 1992.

[7] M. Horowitz and C. R. Menyuk, "Analysis of pulse dropout in harmonically modelocked fiber lasers by use of the Lyapunov method," *Opt. Lett.*, vol. 40, pp. 40–42, 2000.

[8] M. Horowitz, C. R. Menyuk, T. F. Carruthers, and I. N. Duling, III, "Pulse dropout in harmonically modelocked fiber lasers," *IEEE Photon. Technol. Lett.*, vol. 12, no. 3, pp. 266–268, Mar. 2000.

[9] T. Yilmaz, C. M. DePriest, and P. Delfyett Jr., "Complete noise characterisation of external cavity semiconductor laser hybridly modelocked at 10 GHz," *Electron. Lett.*, vol. 37, pp. 1338–1339, 2001.
[10] C. M. DePriest, P. Delfyett Jr., J. H. Abeles, and A. Braun, "Ultra-high-stability photonic sampling streams from an actively-modelocked semiconductor diode ring laser," in *Proc. Conf. Lasers Electro-Optics*, Washington, DC, 2001, pp. 89–90.
[11] J. J. Hargreaves, P. W. Juodawlkis, J. J. Plant, J. P. Donnelly, and J. C. Twichell, "Residual phase-noise measurements of actively modelocked fiber and semiconductor lasers," in *Proc. Annu. Meet. IEEE Lasers and Electro-Optics Soc.*, 2001, pp. 115–116.
[12] F. Rana, H. L. T. Lee, R. J. Ram, E. P. Ippen, and H. A. Haus, "Characterization of the noise and correlations in harmonically mode-locked lasers," *J. Opt. Soc. Amer. B*, vol. 19, pp. 2609–2621, 2002.
[13] F. Rana and R. J. Ram, "Noise and timing jitter in active and hybrid modelocked semiconductor lasers," in *Proc. Conf. Lasers Electro-Optics*, Washington, DC, 2001, pp. 6–7.
[14] D. Von Der Linde, "Characterization of the noise in continuously operating modelocked lasers," *J. Appl. Phys. B*, vol. 39, pp. 201–217, 1986.
[15] H. A. Haus and A. Mecozzi, "Noise of mode-locked lasers," *IEEE J. Quantum Electron.*, vol. 29, no. 3, p. 983, Mar. 1993.
[16] L. A. Coldren and S. Corzine, *Diode Lasers and Photonic Integrated Circuits*. New York: Wiley, 1995.
[17] H. A. Haus, "Theory of mode-locking with a slow saturable absorber," *IEEE J. Quantum Electron.*, vol. 11, no. 8, pt. 1, pp. 736–46, Aug. 1975.
[18] G. F. Franklin, J. D. Powell, and A. Emami-Naeini, *Feedback Control of Dynamic Systems*, 4th ed. Upper Saddle River, NJ: Prentice-Hall, 2002.

Farhan Rana received the B.S., M.S., and Ph.D. degrees from the Massachusetts Institute of Technology (MIT), Cambridge, all in electrical engineering.

He was involved with a variety of different topics related to semiconductor optoelectronics, quantum optics, and mesoscopic physics during his doctoral research. Before starting his doctoral work, he was with IBM's T. J. Watson Research Center, where he was involved with silicon nanocrystal and quantum-dot memory devices. He joined the faculty of the School of Electrical and Computer Engineering, Cornell University, Ithaca, NY, in 2003. His current research focuses on semiconductor optoelctronics and terahertz devices.

Dr. Rana was the recipient of the National Science Foundation Faculty CAREER Award in 2004.

Paul A. George received the B.S. and M.Eng. degrees in electrical and computer engineering from Cornell University, Ithaca, NY, where he is currently working toward the Ph.D. degree in electrical and computer engineering. His master's thesis focused on semiconductor mode-locked lasers.

His current research is focused on ultrafast terahertz photonics and devices.